Percolation, sliding, localization and relaxation in topologically closed circuits

Daniel Hurowitz, Doron Cohen
Department of Physics, Ben-Gurion University of the Negev, Beer-Sheva, Israel

The "glassy" version of *random walk on disordered lattice* features a percolation-related crossover to variable-range-hopping, or to sub-diffusion in one-dimension. The more general problem of *random walk in random environment*, where transition rates are allowed to be asymmetric, has been explored by Sinai, Derrida, and followers. It turns out that for any small amount of disorder an unbiased spreading in one-dimension becomes sub-diffusive, while for bias that exceeds a finite threshold there is a *sliding transition*, leading to a non-zero drift velocity. In the present study we explore the implications of the percolation and sliding transitions for the relaxation modes of a topologically closed circuit. A complementary question regarding the "delocalization" of eigenstates of non-hermitian Hamiltonians has been addressed by Hatano, Nelson, and followers. But we show that for a conservative random-walk dynamics the implied spectral properties are dramatically different.

The original version of Einstein's Brownian motion problem is essentially equivalent to the analysis of a simple *random walk*. The more complicated version is *random walk on a disordered lattice*, which is like a resistor-network problem, involving a percolation-like transition [1]. The latter has diverse applications, e.g. in the context of "glassy" electron dynamics [2, 3]. But more generally one has to consider Sinai's spreading problem [4–7], aka *random walk in a random environment*, that has relevance e.g. for studies in a biophysical context: population biology [8, 9], pulling pinned polymers and DNA denaturation [10, 11] and processive molecular motors [12, 13].

In all these cases the dynamics can be regarded as a stochastic process in which a particle hops from site to site. The rate equation for the site occupation probabilies $\boldsymbol{p} = \{p_n\}$ can be written in matrix notation as

$$\frac{d\boldsymbol{p}}{dt} \;=\; \boldsymbol{W}\boldsymbol{p}, \tag{1}$$

involving a matrix $\boldsymbol{W}$ whose off-diagonal elements are the transitions rates w_{nm}, and with diagonal elements $-\gamma_n$ such that each column sums to zero. Assuming near-neighbor hopping the $\boldsymbol{W}$ matrix takes the form

$$\boldsymbol{W} \;=\; \begin{bmatrix} -\gamma_1 & w_{1,2} & 0 & \ldots \\ w_{2,1} & -\gamma_2 & w_{2,3} & \ldots \\ 0 & w_{3,2} & -\gamma_3 & \ldots \\ \ldots & \ldots & \ldots & \ldots \end{bmatrix} \tag{2}$$

In Einstein's theory $\boldsymbol{W}$ is symmetric, and all the non-zero rates are the same; In the resistor-network problem the rates have some distribution $P(w)$ that features [1]

$$P(w) \;\propto\; w^{\alpha-1} \quad \text{(for small } w\text{)} \tag{3}$$

But in Sinai's problem $\boldsymbol{W}$ is allowed to be asymmetric. Accordingly the rates at the nth bond can be written as $w_n e^{\pm \mathscr{E}_n/2}$ for forward and backward transitions respectively. For the purpose of presentation we assume that the stochastic field $\mathscr{E}$ is box distributed within $[s-\sigma, s+\sigma]$. We refer to s as the bias: it is the pulling force in the case of depinning polymers and DNA denaturation; or the convective flow of bacteria relative to the nutrients in the case of population biology; or the affinity of the chemical cycle in the case of molecular motors.

Our interest is in the relaxation dynamics of finite N-site ring-shaped circuits, that are described by the stochastic equation equation (1). The N sites might be physical locations in some lattice structure, or can represent steps of some chemical-cycle. For example, in the Brownian motor context N is the number of chemical-reactions required to advance the motor one pace. We are inspired by the study of of non-Hermitian quantum Hamiltonians with regard to vortex depinning in type II superconductors [14–16]; molecular motors with *finite* processivity [17, 18]; and related works [19–21]. In both examples conservation of probability is violated. In the first example the bias is the applied transverse magnetic field; and N is the number of defects to which the magnetic vortex can pin.

Scope.– In this article we report how the spectral properties of the matrix $\boldsymbol{W}$ depend on the parameters (α, σ, s), as defined after equation (2). These parameters describe respectively the resistor-network disorder, the stochastic-field disorder, and the average bias field. The eigenvalues $\{-\lambda_k\}$ of $\boldsymbol{W}$ are associated with the relaxation modes of the system. Due to conservation of probability $\lambda_0 = 0$, while all the other eigenvalues $\{\lambda_k\}$ have positive real part, and may have an imaginary part as well. Complex eigenvalues imply that the relaxation is not over-damped: one would be able to observe an oscillating density during relaxation, as demonstrated in Fig.1. The first row of Fig.2 provides some representative spectra. As the bias s is increased a complex bubble appears at the bottom of the band, implying delocalization of the eigenstates. Our results for the complexity threshold s_c are summarized in table I, and demonstrated in Fig.3. The number of complex eigenvalues grows as a function of the bias, as demonstrated in Fig.4, but asymptotically only a finite fraction of the spectrum becomes complex. Our objective below is to explain analytically the peculiarities of this delocalization transition, to explain how it is affected by the percolation and by the sliding thresholds, and to analyze the complexity-saturation effect.

Stochastic spreading.– We first consider an opened ring, namely a disordered chain. The asymmetry can be gauged away, and $\boldsymbol{W}$ becomes similar to a symmetric matrix $\boldsymbol{H}$ (see Methods). The statistics of its off-diagonal elements is characterized by α, while the statistics of the diagonal elements is also affected by σ and s. The eigenvalues $\{-\epsilon_k\}$ of $\boldsymbol{H}$ are real. In the absence of disorder they form a band $[\epsilon_s, \epsilon_\infty]$ where

Type of disorder	Parameters	s_c	Remarks	Figure
Resistor-network disorder	$\alpha<\frac{1}{2},\ \sigma=0$	$s_c=\infty$	non-percolating	
Resistor-network disorder	$\frac{1}{2}<\alpha<1,\ \sigma=0$	$s_c\sim(1/N)$	residual percolation	Fig.3b
Sparse disorder	$(M/N)\ll 1$	$s_c\sim(1/N)$	both disorder types	Fig.3a
Stochastic field disorder	$\alpha>1,\ \sigma\neq 0$	$s_c\approx s_{1/2}$	percolating	Fig.4

TABLE I: **The complexity threshold for different types of disorder**. (Aka delocalization transition). We distinguish between resistor network disorder and stochastic field disorder. The threshold $s_{1/2}$ reflects the strength σ of the latter. It is smaller than the s_1 threshold of the sliding transition. Note that the thresholds s_μ depend neither on N nor on α.

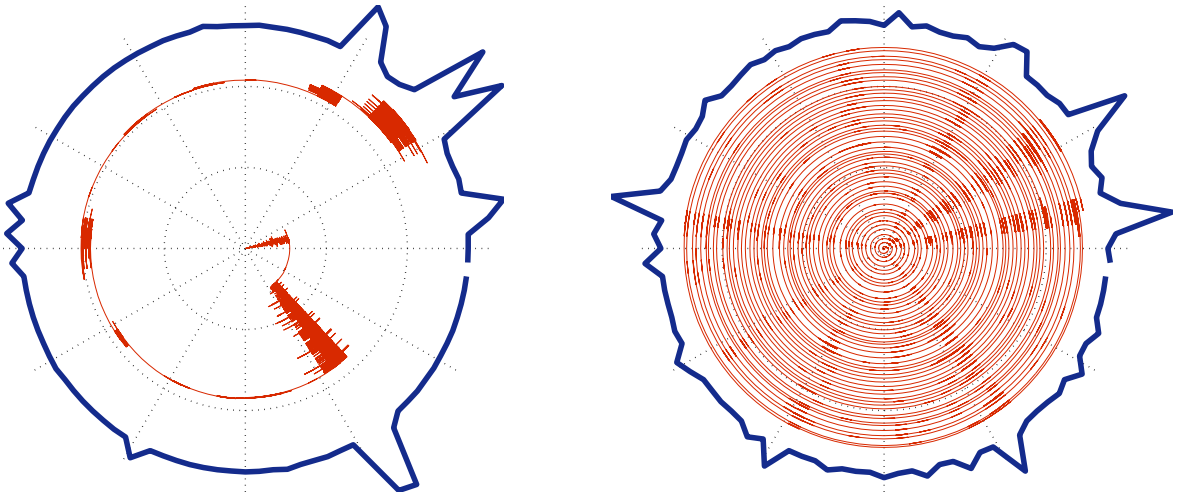

FIG. 1: **Simulated trajectory of a particle on a disordered-ring.** The number of sites is N=100 and the disorder strength is σ=5. The radial direction is time and the angle is the position. For small s (left panel s=0.88) the dynamics is over-damped, while for large s (right panel s=2.97) the dynamics is under-damped. The outer thick line is the steady-state distribution (see Methods).

$\epsilon_{s,\infty}=2[\cosh(s/2)\mp 1]$. For sparse disorder with M ($\ll N$) disordered bonds, a few additional isolated eigenvalues might appear in the gap $[0,\epsilon_s]$. With full disorder it is possible to get a gapless spectrum. This is the case for Gaussian white-noise stochastic-field disorder as analyzed in [6]. In this case there is an analytical expression for the spectral density in terms of Bessel functions. The expression features

$$\rho(\epsilon)\ \propto\ \epsilon^{\mu-1}\quad\text{(for small }\epsilon) \tag{4}$$

with no gap. The exponent is related to the bias via $s=(1/2)\sigma^2\mu$. In the present work we assume the more physically appealing log-box disorder for which (see Methods)

$$s\ =\ s_\mu\ =\ \frac{1}{\mu}\ln\left(\frac{\sinh(\sigma\mu)}{\sigma\mu}\right) \tag{5}$$

Unlike Gaussian disorder the range of possible rates is bounded, and we see that a finite threshold $s_\infty=\sigma$ is deduced. For $s>s_\infty$ a gap opens up. Using the above spectral properties it is deduced that the spreading of a distribution along an infinite chain goes like $x\sim t^\mu$ for $s<s_1$, while for $s>s_1$ we have a non-zero drift velocity. This is known as the "sliding transition". As for the second moment, for $\mu<1/2$ the diffusion coefficient is zero.

The introduction of resistor-network-disorder modifies the spectral density at higher energies, see Fig. 5 for illustration. For $\alpha>1$, in the absence of bias, the continuum-limit approximation features $\mu=1/2$. This reflects a normal diffusive behavior as in Einstein's theory of Brownian motion. Below the percolation threshold, namely for $\alpha<1$, normal diffusion is suppressed, and the spectral exponent is $\mu=\alpha/(1+\alpha)<1/2$. But for large bias, the diagonal disorder in $\boldsymbol{H}$ dominates, leading to trivially localized eigenstates. Hence for large bias we simply have $\mu=\alpha$ irrespective of the percolation aspect.

Relaxation.– We close an N-site chain into a ring. The ring is characterized by its so-called affinity,

$$S_{\circlearrowleft}\ \equiv\ Ns \tag{6}$$

Now a topological aspect is added to the problem, and one wonders what are the relaxation modes of the system. The starting point of our analysis is the secular equation for the eigenvalues of $\boldsymbol{W}$. Assuming that we already know what are the eigenvalues of the associated symmetric matrix $\boldsymbol{H}$, the secular equation takes the form [22]

$$\prod_k\left(\frac{z+\epsilon_k(s)}{\overline{w}}\right)\ =\ 2\left[\cosh\left(\frac{S_{\circlearrowleft}}{2}\right)-1\right] \tag{7}$$

where $\overline{w}$ is the geometric average of all the rates. The bias s affects both the ϵ_k and the right hand side. This equation has

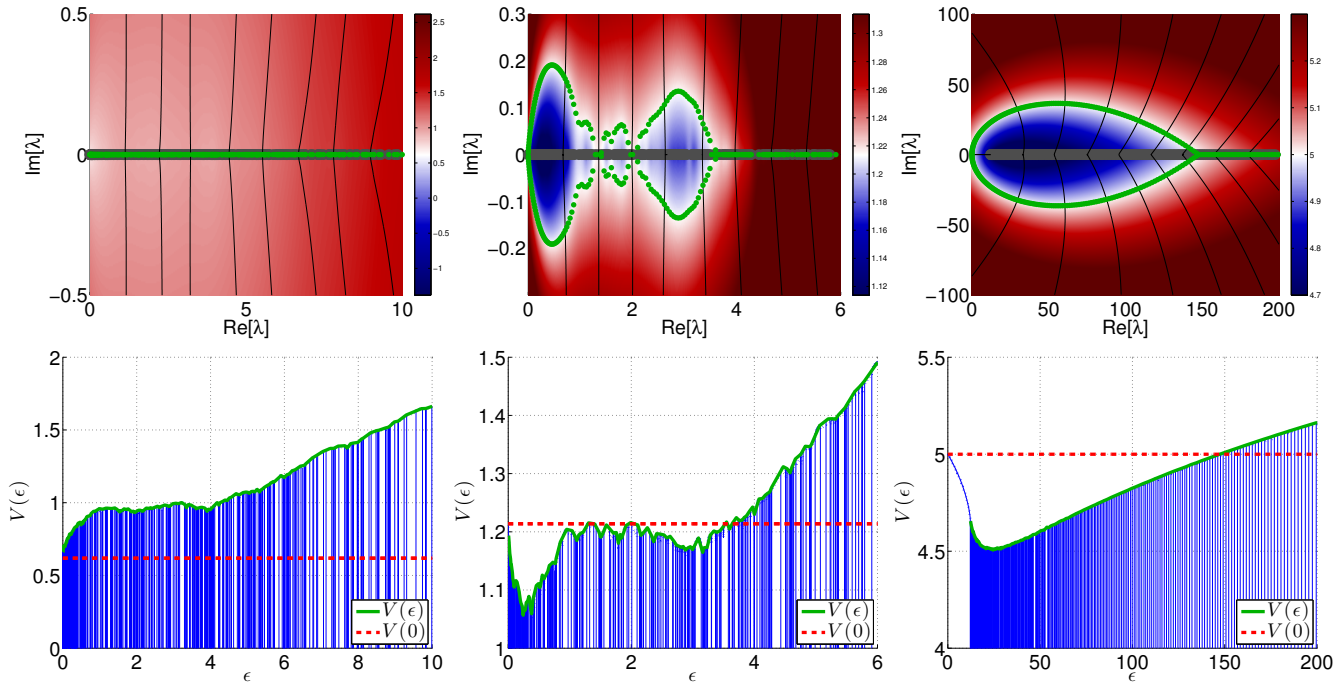

FIG. 2: **The emergence of complexity in the relaxation spectrum.** The upper panels display representative examples of relaxation spectra. The $\{\lambda_k\}$ are indicated by green points in the complex plane. The ring has N=500 sites with σ=5, and (from left to right) $s = 1.24, 2.43, 10$. The calculated threshold values are $s_{1/2} = 1.77$ and $s_1 = 2.7$ and $s_\infty = 5$. In the left hand column $s < s_{1/2}$ and the spectrum is real. In the middle column $s_{1/2} < s < s_\infty$ and the spectrum is with several complex bubbles separated by real segments. In the right column $s > s_\infty$ and the real spectrum has a gap, while the complex spectrum is a fully developed complex bubble, tangent to the origin (no gap). The "electrostatic field" that is associated with the secular equation is represented by a few field-lines, while the background color provides visualization of the corresponding electrostatic potential. The spectrum is obtained by looking for the intersections of the field lines with the equipotential line $V(z) = V(0)$ that goes through the origin (indicated in white). The lower panels plot the potential $V(\epsilon)$ along the real axis. The horizontal dashed line is $V(0)$.

been analyzed in [16] in the case of a non-conservative matrix $\boldsymbol{W}$ whose diagonal elements γ_n are *fixed*, hence the $\epsilon_k(s)$ there do not depend on s. Consequently, as s of equation(6)) is increased beyond a threshold value s_c, the eigenvalues in the middle of the spectrum become complex. As s is further increased beyond some higher threshold value, the entire spectrum becomes complex. As already stated in the introduction, this is not the scenario that is observed for our conservative model. Furthermore we want to clarify how the percolation and sliding thresholds are reflected.

Already at this stage one should be aware of the immediate implications of conservativity. First of all $z = \lambda_0 = 0$ should be a root of the secular equation. The associated eigenstate is the non-equilibrium steady state (NESS), which is an extended state (see Methods). In fact it follows that the localization length has to diverge as $\lambda \to 0$. This is in essence the difference between the conventional Anderson model (Lifshitz tails at the band floor) and the Debye model (phonons at the band floor). It is the latter picture that applies in the case of a conservative model.

Electrostatic picture.– In order to get an insight into the secular equation we define an "electrostatic" potential by taking the log of the left hand side of equation(7). Namely,

$$\Psi(z) \;=\; \sum_k \ln(z-\epsilon_k) \;\equiv\; V(x,y) + iA(x,y) \qquad (8)$$

where $z = x + iy$. Note that we have flipped the sign convention ($z \mapsto -z$), and also we set the time units such that $\overline{w} = 1$. The constant $V(x,y)$ curves correspond to potential contours, and the constant $A(x,y)$ curves corresponds to stream lines. The derivative $\Psi'(z)$ corresponds to the field, which can be regarded as either electric or magnetic field up to a 90deg rotation. Using this language, the secular equation takes the form

$$V(x,y) = V(0); \quad A(x,y) = 2\pi * \text{integer} \qquad (9)$$

Namely the roots are the intersection of the field lines with the potential contour that goes through the origin (Fig.2). We want to find what are the conditions for getting a real spectrum from equation(9), and in particular what is the threshold s_c for getting complex eigenvalues at the bottom of the spectrum. We first look on the potential along the real axis:

$$V(\epsilon) \;=\; \int \ln\left(|\epsilon - x'|\right)\rho(x')dx' \qquad (10)$$

In regions where the $\{\epsilon_k\}$ form a quasi-continuum, one can identify $(1/N)V(\epsilon)$ as the Thouless expression for the inverse

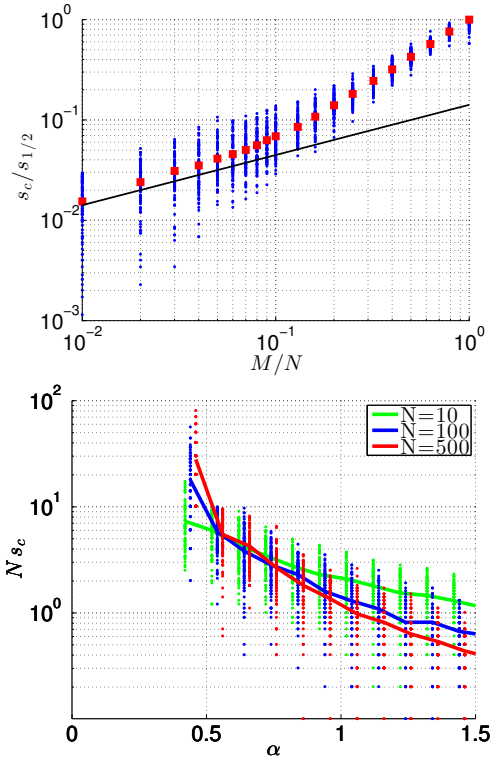

FIG. 3: **The complexity threshold.** Top panel: The threshold value s_c for delocalization versus the number of stochastic field defects M. The number of sites is N=100 and the disorder strength (of the defected sites) is σ=5. Blue dots correspond to different realizations, while red dots are the average (per M). For a fully disordered lattice we expect $s_c = s_{1/2}$, hence the scaling of the axes. The black line is $s_c = M\sigma/N$. Bottom panel: The threshold value s_c versus α. The dots are for different realizations, while the lines are the statistical average. For $\alpha < 1/2$ the s_c diverges as N is increased. Data points for each N are slightly shifted for clarity.

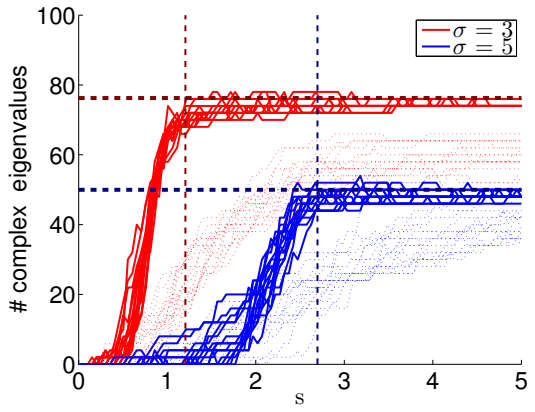

FIG. 4: **Complexity saturation.** The number of complex eigenvalues is counted for a ring with N=100 sites, for various values of the affinity s. Each red line corresponds to a different realization of field disorder with σ=3 (red) and σ=5 (blue). The vertical lines are the corresponding values of s_1, at which the sliding transition occurs. We see that the asymptotic fraction of complex eigenvalues saturates. The horizontal dashed line are the analytical estimates of equation (14). If the lattice were continuous with Gaussian disorder, the number of complex eigenvalues would go to 100%. In the background a disordered resistor network with $\alpha = 0.9$ is shown. The crossover is blurred and the saturation value is lower compared to equation (14).

localization length [16]. The explicit value of $V(0)$ is implied by equation (7), namely $V(0) = \ln[2(\cosh(S_\circlearrowleft/2) - 1)]$. For a charge-density that is given by equation (4), with some cutoff ϵ_c, the derivative of the electrostatic potential at the origin is (see Methods)

$$V'(\epsilon) \approx \frac{\epsilon^{\mu-1}}{\epsilon_c^{\mu}} \pi\mu \cot(\pi\mu) \qquad (11)$$

One observes that the sign changes from positive to negative at $\mu = 1/2$. Some examples are illustrated in Fig.2. Clearly, if the envelope of $V(\epsilon)$ is above the $V = V(0)$ line, then the spectrum is real, and the λ_k are roughly the same as the ϵ_k, shifted a bit to the left.

From the above it follows that the threshold s_c for the appearance of a complex quasi-continuum is either $V(\epsilon_s) < V(0)$ or $V'(0) < 0$, depending on whether $\rho(\epsilon)$ is gapped or not. In the latter case it follows from equation (11) that $s_c = s_{1/2}$. We note that for the Gaussian model of [6] one obtains $V(\epsilon \to \infty) = \text{const}$, implying that the entire spectrum would go from real to complex at $s = s_{1/2}$. In general this is not the case: the complex spectrum typically forms a "bubble" tangent to the origin, or possibly one may find some additional bubbles as in Fig.2b.

The identification of the s_c with $s_{1/2}$ holds for full disorder, but not for sparse disorder. In the latter case $s_c \propto 1/N$, or we may better look on $S_c = Ns_c$. The reasoning that leads to this conclusion is as follows: We start with a clean ring. Recall that $\rho(\epsilon)$ feature a gap $[0, \epsilon_s]$. If we have M defected bonds with some σ disorder the condition $V(\epsilon_s) < V(0)$ implies $S_c = M\sigma$ (see methods). The handling of weak links is a bit more complicated (see Methods) but leads to the same conclusion, where the role of σ is played by the dispersion of the defected w_n.

Complexity saturation.– The secular equation for the eigenvalues is given by equation (7). In the nonconservative case, the eigenvalues of $\boldsymbol{H}$ do not depend on s, thus raising s will eventually make the entire spectrum complex. For a conservative matrix, however, $V(\epsilon)$ is also a function of s, so increasing s raises $V(\epsilon)$ at the same rate. Taking s to be as large as desired, the eigenvalues of H become trivially $\gamma_n = w_n e^{\mathscr{E}_n/2}$, and the equation $V(\epsilon) = V(0)$ for the upper cutoff ϵ_c of the complex energies takes the form

$$\overline{\ln\left[\epsilon - we^{\mathscr{E}/2}\right]} \;=\; s/2 \qquad (12)$$

It is natural to write the stochastic field as $\mathscr{E} = s + \varsigma$, such that $\varsigma \in [-\sigma, +\sigma]$. For the purpose of presentation we assume that w=1. Then the spectrum stretches from $\epsilon_s = e^{(s-\sigma)/2}$ to $\epsilon_c = e^{(s+\sigma_c)/2}$, where σ_c is the solution of

$$\int_{-\sigma}^{\sigma} \ln\left|e^{\varsigma/2} - e^{\sigma_c/2}\right| d\varsigma \;=\; 0 \qquad (13)$$

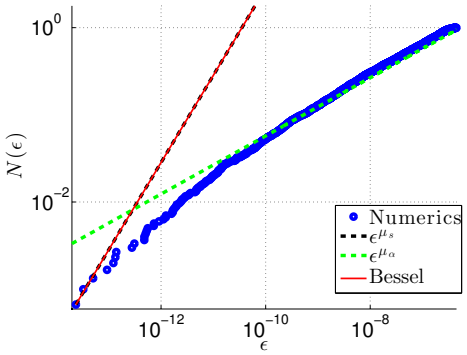

FIG. 5: **The spectrum of the associated hermitian matrix.** We calculate numerically the integrated density, which counts the eigenvalues $\{\epsilon_k < \epsilon\}$ of $\boldsymbol{H}$ for a ring with N=3000 sites. The system is characterized by a percolation exponent $\mu = \mu_\alpha = 1/3$, and by a scaled affinity $\mu = \mu_s = 1$. The stochastic-field distribution is with σ=2. The blue points are are results of numerical diagonalization. There is a crossover from density that corresponds to μ_s (dashed black line), to density that corresponds to μ_α (dashed green line). The red line is the Bessel expression of [6].

It follows that the fraction of complex eigenvalues is

$$\text{fraction} = \frac{1}{N}\int_{\epsilon_s}^{\epsilon_c} \rho(\epsilon)d\epsilon = \frac{1}{\sigma}\ln\left(\frac{\epsilon_c}{\epsilon_s}\right) = \frac{\sigma_c+\sigma}{2\sigma} \tag{14}$$

We demonstrate the agreement with this formula in Fig.4. We plot there also what happens if resistor-network disorder is introduced. We see that for small α the crossover is not as sharp and the saturation value is lower than equation (14) as expected from equation (12).

In conclusion.– we have shown that the relaxation properties of a closed circuit (or chemical-cycle), whose dynamics is generated by a conservative rate-equation, is dramatically different from that of a biased non-hermitian Hamiltonian. The transition to complexity depends on the type of disorder as summarized in table I. Surprisingly it happens for $\alpha > 1/2$ before the percolation transition, and for $\mu > 1/2$ before the sliding transition, and diminishes as $1/N$ for sparse disorder. Further increasing the bias does not lead to full delocalization, instead a "complexity saturation" is observed.

I. METHODS

The NESS formula.– Following the derivation in [23] the explicit formula for the NESS is

$$p_n \propto \left(\frac{1}{w_{\vec{n}}}\right)_s e^{-(U(n)-U_s(n))} \tag{15}$$

where $U(n)$ is the stochastic potential that is associated with the field $\mathscr{E}_n$, the transitions in the drift-wise direction are $w_{\vec{n}} = w_n e^{\mathscr{E}_n/2}$, and the subscript s indicates drift-wise smoothing over a length scale $1/s$. Note that in the absence of bias the smoothed functions are constant and we get the canonical equilibrium state.

The similarity transformation.– Define the diagonal matrix $\boldsymbol{U} = \text{diag}\{U(n)\}$. The stochastic field can be made uniform, as in [16], by performing a similarity transformation $\tilde{\boldsymbol{W}} = e^{\boldsymbol{U}/2}\boldsymbol{W}e^{-\boldsymbol{U}/2}$, leading to

$$\tilde{\boldsymbol{W}} \;=\; \text{diagonal}\Big\{-\gamma_n\Big\} + \text{offdiagonal}\Big\{w_n e^{\pm\frac{S_\circlearrowleft}{2N}}\Big\} \tag{16}$$

where the "±" are for the forward and backward transitions respectively. Note that the s-dependent statistics of the $\mathscr{E}_n$ is still hiding in the diagonal elements. The associated symmetric matrix $\boldsymbol{H}$ is defined by setting $S_\circlearrowleft = 0$. Then one can define an associated spectrum ϵ_k. For an open chain setting $S_\circlearrowleft = 0$ can be regarded as a gauge transformation of an imaginary vector potential. For a closed ring $S_\circlearrowleft$ is like an imaginary Aharonov-Bohm flux, and cannot be gauged away.

Finding s_μ.– The cummulant generating function of the stochastic field can be written as $g(\mu) = (s - s_\mu)\mu$, where the s_μ are defined via the following expression:

$$\left\langle e^{-\mathscr{E}\mu}\right\rangle \;\equiv\; e^{-(s-s_\mu)\mu} \tag{17}$$

If the stochastic field has normal distribution with standard deviation σ, then $s_\mu = (1/2)\sigma^2\mu$. For our log-box distribution equation (5) applies. The finite value of s_∞ reflects that $\mathscr{E}$ is bounded.

Finding $V'(0)$.– To derive equation (11) we assume an integrated density of states that corresponds to equation (4), namely, $\mathscr{N}(\epsilon) = (\epsilon/\epsilon_c)^\mu$, where ϵ_c is some cutoff that reflects the discreteness of the lattice. After integration by parts the electrostatic potential along the real axis is given by

$$V(\epsilon) \;=\; -\int_0^{\epsilon_c} \frac{\mathscr{N}(x)}{x-\epsilon}dx \tag{18}$$

While calculating the derivative we assume $\epsilon \ll \epsilon_c$, hence taking the upper limit of the scaled integral as infinity:

$$V'(\epsilon) \;=\; \frac{\mu}{\epsilon_c^\mu}\epsilon^{\mu-1}\int_0^\infty \frac{z^{\mu-1}}{z-1}dz \tag{19}$$

$$\;=\; -\frac{\mu}{\epsilon_c^\mu}\epsilon^{\mu-1}\,B_\infty(\mu,0) \tag{20}$$

where $B_u(a,b)$ is the Incomplete Euler Beta function. Taking the Cauchy principal part we get

$$B_\infty(\mu,0) \;=\; \lim_{\delta\to 0}\left[B_{1-\delta}(\mu,0) - B_{1-\delta}(1-\mu,0)\right] \tag{21}$$

$$\;=\; \psi(1-\mu) - \psi(\mu) = \pi\cot(\pi\mu) \tag{22}$$

where $\psi(z)$ is the digamma function, and the last equality has been obtained by the reflection formula.

Finding s_c due to a biased-link.– We consider a clean ring. We assume that the stochastic field over one bond is exceptionally large compared to all other bonds. Then there

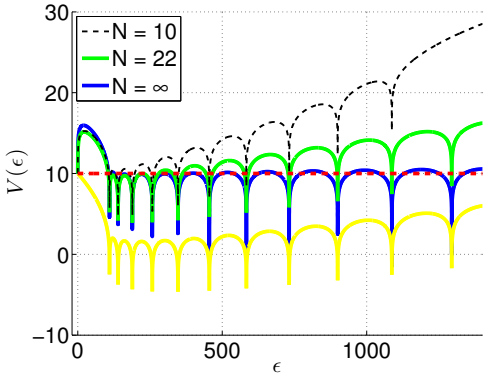

FIG. 6: **Graphical illustration of the the secular equation for a ring with a weak link.** The red line is $V(0) = \ln[2(\cosh(S_{\circlearrowleft}/2) - 1)]$. The blue line is $V(\epsilon)$ as deduced from the LHS of equation (23) with $L = 1$, $g = 10^{-3}$ and $S_{\circlearrowleft} = 20$. The yellow line is an attempted reconstruction of $V(\epsilon)$ from the first $N = 22$ roots ϵ_k of the $S_{\circlearrowleft}$=0 equation. The green line is a proper reconstruction that takes into account an impurity term ϵ_0. The deviation from the blue line for large k is due to finite truncation: compare the N=10 line with the N=22 line.

is an extra "impurity" level $\epsilon_1 \approx \gamma_1 \approx \exp[(s+\sigma)/2]$ that is located above the continuum of extended modes. The contribution of this impurity to $V(\epsilon_s)$ is $\ln(\epsilon_s - \gamma_1)$. The contribution of the continuum can be neglected due to the Thouless relation. Hence the condition $V(\epsilon_s) > V(0)$ implies $s_c \approx \sigma/N$.

Finding s_c due to a weak-link.– We consider a clean ring of length $L = Na$ with lattice spacing a and identical bonds ($w_n = 1$). We change one bond into a weak link ($w_1 \ll 1$). This setup can be treated exactly in the continuum limit, where equation (1) corresponds to a diffusion equation with coefficient $D_0 = wa^2$ and drift velocity $v_0 = swa$. The weak link corresponds to a segment where the diffusion coefficient is $D_1 \ll D_0$. Using transfer matrix methods we find the secular equation

$$\cos(k) + \frac{1}{g}\frac{k^2 + \left(\frac{S_{\circlearrowleft}}{2}\right)^2}{2k}\sin(k) \;=\; \cosh\left(\frac{S_{\circlearrowleft}}{2}\right) \qquad (23)$$

where $k^2 = (L^2/D)z - (S_{\circlearrowleft}/2)^2$, and $g = (D_1/a)/(D_0/L)$. We have taken here the limit $a \to 0$, keeping $(L, g, S_{\circlearrowleft})$ constant. The equation is graphically illustrated in Fig.6. All the roots are real solutions provided the envelope of the left-hand-side (LHS) lays above the right-hand-side (RHS). The minimum of the envelope of the LHS is obtained at $z = S_{\circlearrowleft}^2/2$. Consequently we find that the threshold S_c obeys

$$\frac{S_{\circlearrowleft}}{2g} \;=\; \cosh\left[\frac{S_{\circlearrowleft}}{2}\right] \qquad (24)$$

provided $S_{\circlearrowleft} \gg g$, which is self-justified for small g. The solution is given in terms of the Lambert function, namely $S_c = -2\mathbb{W}(-g/2)$, leading to $s_c = S_c/N$.

The secular, equation equation (23), parallels the discrete version equation (7), with a small twist that we would like to point out. Naively one would like to identify $\ln[2(\mathrm{LHS} - 1)]$, up to a constant, with $\sum_{k=1}^{\infty} \ln(\epsilon - \epsilon_k)$, where the ϵ_k are the roots of equation (23) with $S_{\circlearrowleft}$=0 in the RHS. This is tested in Fig.6, and we see that there is a problem. Then one realizes that in fact an additional $k = 0$ term with $0 \lesssim \epsilon_0 < \epsilon_s$ is missing. Going back to the discrete version it corresponds to an impurity-level that is associated with a mode which is located at the weak-link. While taking the limit $a \to 0$ this level becomes excluded. Adding it back we we see that the agreement between equation (7) and equation (23) is restored. The residual systematic error as k becomes larger is due to finite truncation of the number of roots used in the reconstruction. Making the approximation $\ln(\epsilon_s - \epsilon_0) \approx \ln[(s/2)^2]$, and noting that $g \propto N$, it is verified that the equation $V(\epsilon_s) = V(0)$ for the complexity threshold is consistent with equation (24).

[1] Alexander, S., Bernasconi, J., Schneider, W. R. & Orbach, R. Excitation dynamics in random one-dimensional systems. *Rev. Mod. Phys.* **53**, 175–198 (1981). URL `http://link.aps.org/doi/10.1103/RevModPhys.53.175`.

[2] Vaknin, A., Ovadyahu, Z. & Pollak, M. Aging effects in an anderson insulator. *Phys. Rev. Lett.* **84**, 3402–3405 (2000). URL `http://link.aps.org/doi/10.1103/PhysRevLett.84.3402`.

[3] Amir, A., Oreg, Y. & Imry, Y. Slow relaxations and aging in the electron glass. *Phys. Rev. Lett.* **103**, 126403 (2009). URL `http://link.aps.org/doi/10.1103/PhysRevLett.103.126403`.

[4] Sinai, Y. G. The limiting behavior of a one-dimensional random walk in a random medium. *Theory of Probability & Its Applications* **27**, 256–268 (1983). URL `http://dx.doi.org/10.1137/1127028`. http://dx.doi.org/10.1137/1127028.

[5] Derrida, B. Velocity and diffusion constant of a periodic one-dimensional hopping model. *Journal of Statistical Physics* **31**, 433–450 (1983). URL `http://dx.doi.org/10.1007/BF01019492`.

[6] Bouchaud, J., Comtet, A., Georges, A. & Doussal, P. L. Classical diffusion of a particle in a one-dimensional random force field. *Annals of Physics* **201**, 285 – 341 (1990). URL `http://www.sciencedirect.com/science/article/pii/000349169090043N`.

[7] Bouchaud, J.-P. & Georges, A. Anomalous diffusion in disordered media: Statistical mechanisms, models and physical applications. *Physics Reports* **195**, 127 – 293 (1990). URL `http://www.sciencedirect.com/science/article/pii/037015739090099N`.

[8] Nelson, D. R. & Shnerb, N. M. Non-hermitian localization and population biology. *Phys. Rev. E* **58**, 1383–1403 (1998). URL `http://link.aps.org/doi/10.1103/PhysRevE.58.1383`.

[9] Dahmen, K. A., Nelson, D. R. & Shnerb, N. M. Population dynamics and non-hermitian localization. In *Statistical mechanics*

of biocomplexity, 124–151 (Springer, 1999).

[10] Lubensky, D. K. & Nelson, D. R. Pulling pinned polymers and unzipping dna. *Phys. Rev. Lett.* **85**, 1572–1575 (2000). URL http://link.aps.org/doi/10.1103/PhysRevLett.85.1572.

[11] Lubensky, D. K. & Nelson, D. R. Single molecule statistics and the polynucleotide unzipping transition. *Phys. Rev. E* **65**, 031917 (2002). URL http://link.aps.org/doi/10.1103/PhysRevE.65.031917.

[12] Fisher, M. E. & Kolomeisky, A. B. The force exerted by a molecular motor. *Proceedings of the National Academy of Sciences* **96**, 6597–6602 (1999).

[13] Rief, M. *et al.* Myosin-v stepping kinetics: a molecular model for processivity. *Proceedings of the National Academy of Sciences* **97**, 9482–9486 (2000).

[14] Hatano, N. & Nelson, D. R. Localization transitions in non-hermitian quantum mechanics. *Phys. Rev. Lett.* **77**, 570–573 (1996). URL http://link.aps.org/doi/10.1103/PhysRevLett.77.570.

[15] Hatano, N. & Nelson, D. R. Vortex pinning and non-hermitian quantum mechanics. *Phys. Rev. B* **56**, 8651–8673 (1997). URL http://link.aps.org/doi/10.1103/PhysRevB.56.8651.

[16] Shnerb, N. M. & Nelson, D. R. Winding numbers, complex currents, and non-hermitian localization. *Phys. Rev. Lett.* **80**, 5172–5175 (1998). URL http://link.aps.org/doi/10.1103/PhysRevLett.80.5172.

[17] Kafri, Y., Lubensky, D. K. & Nelson, D. R. Dynamics of molecular motors and polymer translocation with sequence heterogeneity. *Biophysical Journal* **86**, 3373 – 3391 (2004). URL http://www.sciencedirect.com/science/article/pii/S0006349504743854.

[18] Kafri, Y., Lubensky, D. K. & Nelson, D. R. Dynamics of molecular motors with finite processivity on heterogeneous tracks. *Phys. Rev. E* **71**, 041906 (2005). URL http://link.aps.org/doi/10.1103/PhysRevE.71.041906.

[19] Brouwer, P. W., Silvestrov, P. G. & Beenakker, C. W. J. Theory of directed localization in one dimension. *Phys. Rev. B* **56**, R4333–R4335 (1997). URL http://link.aps.org/doi/10.1103/PhysRevB.56.R4333.

[20] Goldsheid, I. Y. & Khoruzhenko, B. A. Distribution of eigenvalues in non-hermitian anderson models. *Phys. Rev. Lett.* **80**, 2897–2900 (1998). URL http://link.aps.org/doi/10.1103/PhysRevLett.80.2897.

[21] Feinberg, J. & Zee, A. Non-hermitian localization and delocalization. *Phys. Rev. E* **59**, 6433–6443 (1999). URL http://link.aps.org/doi/10.1103/PhysRevE.59.6433.

[22] Molinari, L. G. Determinants of block tridiagonal matrices. *Linear Algebra and its Applications* **429**, 2221 – 2226 (2008). URL http://www.sciencedirect.com/science/article/pii/S0024379508003200.

[23] Hurowitz, D. & Cohen, D. Nonequilibrium version of the einstein relation. *Phys. Rev. E* **90**, 032129 (2014). URL http://link.aps.org/doi/10.1103/PhysRevE.90.032129.

Acknowledgements

This research has been supported by by the Israel Science Foundation (grant No. 29/11).